Evidence for the Strangeness-Changing Weak Decay $\Xi_b^- \to \Lambda_b^0 \pi^-$

R. Aaij *et al.*[*]
(LHCb Collaboration)

(Received 13 October 2015; published 11 December 2015)

Using a pp collision data sample corresponding to an integrated luminosity of 3.0 fb^{-1}, collected by the LHCb detector, we present the first search for the strangeness-changing weak decay $\Xi_b^- \to \Lambda_b^0 \pi^-$. No b hadron decay of this type has been seen before. A signal for this decay, corresponding to a significance of 3.2 standard deviations, is reported. The relative rate is measured to be

$$\frac{f_{\Xi_b^-}}{f_{\Lambda_b^0}} \mathcal{B}(\Xi_b^- \to \Lambda_b^0 \pi^-) = (5.7 \pm 1.8^{+0.8}_{-0.9}) \times 10^{-4},$$

where $f_{\Xi_b^-}$ and $f_{\Lambda_b^0}$ are the $b \to \Xi_b^-$ and $b \to \Lambda_b^0$ fragmentation fractions, and $\mathcal{B}(\Xi_b^- \to \Lambda_b^0 \pi^-)$ is the branching fraction. Assuming $f_{\Xi_b^-}/f_{\Lambda_b^0}$ is bounded between 0.1 and 0.3, the branching fraction $\mathcal{B}(\Xi_b^- \to \Lambda_b^0 \pi^-)$ would lie in the range from $(0.57 \pm 0.21)\%$ to $(0.19 \pm 0.07)\%$.

DOI: 10.1103/PhysRevLett.115.241801 PACS numbers: 13.30.Eg

Measurements of the lifetimes of beauty baryons provide an important test of heavy-quark effective theory (HQET) [1–8] in which it is predicted that the decay width is dominated by the weak decay of the heavy b quark. Large samples of b baryons have been collected by LHCb, enabling precise measurements of their masses and lifetimes [9–12], which are generally in good agreement with HQET predictions. Recently, it has been noted [13–16] that for the Ξ_b^- and Ξ_b^0 baryons, the weak decay of the s quark could contribute about 1% to the total decay width. It has also been argued [13] that if the light diquark system has $J^P = 0^+$ and exhibits the diquark correlations suggested in Refs. [17,18], this could enhance the contribution from the weak decay of the s quark in the Ξ_b^- (Ξ_b^0) baryon to a level that ranges from 2% to 8% (1% to 4%). Such a large rate would affect the comparison between HQET predictions and measurements of the Ξ_b^- and Ξ_b^0 lifetimes.

These ideas can be tested by studying the decay $\Xi_b^- \to \Lambda_b^0 \pi^-$, in which the s quark in the $\Xi_b^-(bds)$ undergoes a $s \to u\bar{u}d$ weak transition to a Λ_b^0 (bud) baryon and a π^- meson. A measurement of the rate of this process would provide valuable experimental input on the size of the aforementioned contributions to the Ξ_b^- decay width, as well as on the $J^P = 0^+$ diquark potential.

We present a search for the decay $\Xi_b^- \to \Lambda_b^0 \pi^-$, where the Λ_b^0 baryon is reconstructed through its decay to $\Lambda_c^+ \pi^-$, with $\Lambda_c^+ \to pK^-\pi^+$. The signal yield is normalized with respect to the total number of Λ_b^0 decays reconstructed in the same final state. Charge conjugate processes are implied throughout. The quantity that is measured is

$$r_s \equiv \frac{f_{\Xi_b^-}}{f_{\Lambda_b^0}} \mathcal{B}(\Xi_b^- \to \Lambda_b^0 \pi^-) = \frac{N(\Xi_b^- \to \Lambda_b^0 \pi^-)}{N(\Lambda_b^0)} \epsilon_{\rm rel} \quad (1)$$

where $f_{\Xi_b^-}$ and $f_{\Lambda_b^0}$ are the $b \to \Xi_b^-$ and $b \to \Lambda_b^0$ fragmentation fractions, $N(\Xi_b^- \to \Lambda_b^0 \pi^-)$ and $N(\Lambda_b^0)$ are the signal yields, and $\epsilon_{\rm rel}$ is the relative efficiency between the normalization and signal modes. The signal for the $\Xi_b^- \to \Lambda_b^0 \pi^-$ decay is a narrow peak at 38.8 ± 0.5 MeV/c^2 [12] in the spectrum of the mass difference, $\delta m \equiv M(\Lambda_b^0 \pi^-) - M(\Lambda_b^0) - m_\pi$, where $M(\Lambda_b^0 \pi^-)$ and $M(\Lambda_b^0)$ are the invariant masses of the respective candidates, and m_π is the π^- mass [19].

The measurement uses proton-proton (pp) collision data samples collected by the LHCb experiment, corresponding to an integrated luminosity of 3.0 fb^{-1}, of which 1.0 fb^{-1} was recorded at a center-of-mass energy of 7 TeV and 2.0 fb^{-1} at 8 TeV.

The LHCb detector [20] is a single-arm forward spectrometer covering the pseudorapidity range $2 < \eta < 5$, designed for the study of particles containing b or c quarks. The detector includes a high-precision tracking system, which provides a momentum measurement with relative uncertainty of about 0.5% from 2–100 GeV/c and an impact parameter resolution of 20 μm for particles with large transverse momentum (p_T). The polarity of the dipole magnet is reversed periodically throughout the taking of data to reduce asymmetries in the detection of charged

[*]Full author list given at the end of the article.

particles. Ring-imaging Cherenkov detectors [21] are used to distinguish different types of charged hadrons. Photon, electron, and hadron candidates are identified using a calorimeter system, which is followed by detectors to identify muons [22].

The trigger [23] consists of a hardware stage, based on information from the calorimeter and muon systems, and a software stage, which applies a full event reconstruction [23,24]. The software trigger requires a two-, three-, or four-track secondary vertex that is significantly displaced from the primary pp interaction vertices (PVs) and whose tracks have a large scalar p_T sum. At least one track should have $p_T > 1.7$ GeV/c and be inconsistent with coming from any of the PVs. The signal candidates are also required to pass a multivariate software trigger selection algorithm [24].

Proton-proton collisions are simulated using PYTHIA [25] with a specific LHCb configuration [26]. Decays of hadronic particles are described by EVTGEN [27], in which final-state radiation is generated using PHOTOS [28]. The interaction of the generated particles with the detector, and its response, are implemented using the GEANT4 toolkit [29] as described in Ref. [30].

Candidate Λ_b^0 decays are formed by combining $\Lambda_c^+ \to pK^-\pi^+$ and π^- candidates in a kinematic fit [31]. The selection criteria are identical to those used in Ref. [12], except that no requirement is made on the particle identification (PID) information for the π^- candidate. For each combination of a Λ_b^0 candidate and a PV in the event, the quantity $\chi^2_{\rm IP}$ is computed, defined to be the difference in χ^2 of the PV fit when the Λ_b^0 particle is included or excluded from the fit. The Λ_b^0 candidate is assigned to the PV with the smallest $\chi^2_{\rm IP}$.

Right-sign (RS) $\Xi_b^- \to \Lambda_b^0\pi^-$ candidates are obtained by combining a Λ_b^0 candidate with mass in the range 5560–5680 MeV/c^2 with a π^- candidate, and wrong-sign (WS) candidates are likewise formed from $\Lambda_b^0\pi^+$ combinations. The pions are required to have $p_T > 100$ MeV/c, and to have PID information consistent with a $\pi^\pm$ meson. Because these pions are generally consistent with emanating from the PV, the PID requirement helps to suppress background from other particle types. A second kinematic fit is used to compute δm; it exploits both vertex and invariant mass constraints, requiring for the latter that the invariant masses of the $pK^-\pi^+$ and $\Lambda_c^+\pi^-$ systems are equal to the known Λ_c^+ and Λ_b^0 masses.

Three boosted decision tree (BDT) multivariate discriminants [32,33] are used to suppress background, one for the normalization mode (BDT1), and two for the signal mode (BDT2 and BDT3). BDT1 is used specifically to suppress the combinatorial background contribution in the Λ_b^0 normalization mode. Five input variables are used: the χ^2 of the Λ_b^0 kinematic fit, the $\chi^2_{\rm IP}$ of the Λ_b^0, Λ_c^+, and π^- candidates, and the $\chi^2_{\rm VS}$ of the Λ_b^0 candidate. Here, $\chi^2_{\rm VS}$ is the difference between the χ^2 of the PV fit with and without the Λ_b^0 daughter particles included in the fit. A large $\chi^2_{\rm VS}$ indicates that the Λ_b^0 decay vertex is well separated from its associated PV. Simulated $\Lambda_b^0 \to \Lambda_c^+\pi^-$ decays are used to model the signal distributions of the BDT1 input variables, and candidates with $M(\Lambda_c^+\pi^-) > 5700$ MeV/c^2 are used to model the corresponding background spectra. A loose selection on the BDT1 output is applied, which provides an efficiency of $(98.6 \pm 0.5)\%$, while reducing the background by a factor of four.

The invariant mass spectrum of selected $\Lambda_c^+\pi^-$ candidates is displayed in Fig. 1. The yield is determined from an unbinned extended maximum likelihood fit using the signal and background shapes as described in Ref. [11]. The fitted number of $\Lambda_b^0 \to \Lambda_c^+\pi^-$ decays is $(256.7 \pm 0.6) \times 10^3$, and the fraction $N(\Lambda_b^0 \to \Lambda_c^+K^-)/N(\Lambda_b^0 \to \Lambda_c^+\pi^-) = (5.9 \pm 0.2)\%$, where the uncertainties are statistical only. In the mass region 5560–5680 MeV/c^2, the fitted yields of $\Lambda_b^0 \to \Lambda_c^+\pi^-$ and $\Lambda_b^0 \to \Lambda_c^+K^-$ decays are 253 300 and 11 700, respectively. Since misidentified $\Lambda_b^0 \to \Lambda_c^+K^-$ signal decays also contribute to the $\Xi_b^- \to \Lambda_b^0\pi^-$ signal, they are included in the total normalization mode yield. Thus, the signal yield for the normalization mode is $(265 \pm 1) \times 10^3$.

The second BDT (BDT2) has the same purpose as BDT1, except that it is applied to the Λ_b^0 candidates within the $\Xi_b^- \to \Lambda_b^0\pi^-$ sample. This alternate BDT is needed since the lifetime of the Ξ_b^- baryon is about the same as that of the Λ_b^0 baryon, thus leading to larger typical values of $\chi^2_{\rm VS}$ compared to the inclusively produced Λ_b^0 sample. A similar training to that of BDT1 is performed, except that the signal distributions are taken from simulated $\Xi_b^- \to \Lambda_b^0\pi^-$ decays. A loose selection on the BDT2 output yields an efficiency of $(99.0 \pm 0.5)\%$.

The third BDT (BDT3) is used to distinguish real $\Xi_b^- \to \Lambda_b^0\pi^-$ decays from Λ_b^0 baryons combined with a

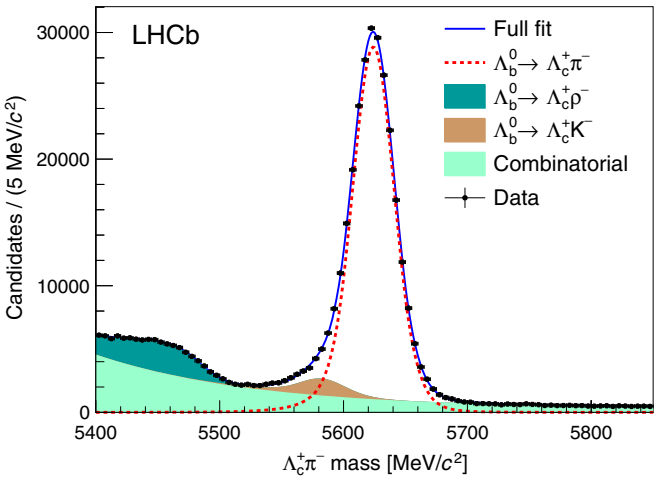

FIG. 1 (color online). Invariant mass spectrum for selected $\Lambda_b^0 \to \Lambda_c^+\pi^-$ candidates in data.

random π^- candidate. Because of the small energy release in the $\Xi_b^- \to \Lambda_b^0 \pi^-$ decay, the Λ_b^0 and π^- directions are nearly collinear with that of the Ξ_b^-. This makes it difficult to identify the Λ_b^0 and π^- daughters as particles produced at a secondary vertex. The input variables used in BDT3 are the flight distance and $\chi^2_{\rm VS}$ of the Ξ_b^- candidate, the $\chi^2_{\rm VS}$ of the Λ_b^0 candidate, and the $\chi^2_{\rm IP}$ and p_T of the low-momentum (slow) π^- daughter of the Ξ_b^- candidate. The signal distributions of these variables are taken from simulated $\Xi_b^- \to \Lambda_b^0 \pi^-$ decays, and the background spectra are taken from WS candidates that have $34 < \delta m < 44$ MeV/c^2. Separate training and test samples were compared and showed no bias due to overtraining.

A loose selection on the BDT3 output is applied, rejecting about 3% of the expected signal events. The selected events are divided into two signal-to-background (S/B) regions according to the BDT3 output: a high-S/B region and a low-S/B region. The split between the high- and low-S/B regions is chosen to provide optimal expected sensitivity. The expected ratio of yields in the low-S/B to high-S/B regions is 1.60, which is fixed in the fit to data.

An event may have more than one Ξ_b^- candidate; this is almost always due to a single Λ_b^0 candidate being combined with more than one π^- candidate. The average number of candidates in events that contain a candidate in the low-S/B region is 1.35, and 1.02 in events that contain a candidate in the high-S/B region. All candidates are kept. Potential bias on the signal yield determination due to this choice was investigated, and none was found.

Four disjoint subsamples of data are used in the fits, split by charge (RS, WS) and by S/B region (low, high). Including the WS data allows additional constraints on the shape of the combinatorial background, and also provides a consistency check that the signal yield in the $\Lambda_b^0 \pi^+$ mode is consistent with zero. In these four δm spectra we allow for three contributions: a $\Xi_b^- \to \Lambda_b^0 \pi^-$ signal, strong decays of $\Sigma_b^{(*)\pm} \to \Lambda_b^0 \pi^\pm$ resonances, and combinatorial background. The low-S/B region contains almost all of the $\Sigma_b^{(*)\pm} \to \Lambda_b^0 \pi^\pm$ signal decays. The primary reason for including the low-S/B regions is that they contain almost all of the $\Sigma_b^{(*)\pm} \to \Lambda_b^0 \pi^\pm$ signal decays. This leads to tighter constraints on the $\Sigma_b^{(*)\pm} \to \Lambda_b^0 \pi^\pm$ mass shapes in the high-S/B region, since the shape parameters are common to the low- and high-S/B regions. A simultaneous unbinned extended maximum likelihood fit is performed to the four δm spectra, in the range 2–122 MeV/c^2, using the signal and background shapes discussed below.

The δm signal shape is obtained from simulated $\Xi_b^- \to \Lambda_b^0 \pi^-$ decays, allowing for different signal shapes in the low- and high-S/B regions. Each sample is fit to the sum of two Gaussian functions with a common mean value. The shapes are slightly different, but the average resolution, given as the weighted average of the two Gaussian widths, is 1.57 MeV/c^2 in both cases. All signal shape parameters are fixed in fits to data, including the mean, which is fixed to $M(\Xi_b^-) - M(\Lambda_b^0) - m_{\pi^-} = 38.8$ MeV/c^2 [12]. A scale factor of 1.10 is applied to the widths to account for slightly worse resolution in data than simulation, as determined from a study of the δm resolution in $D^{*+} \to D^0 \pi^+$ decays [34]. Variations in this value are considered as a source of systematic uncertainty.

The contributions from the $\Sigma_b^\pm$ and $\Sigma_b^{*\pm}$ resonances are each modeled using a relativistic Breit Wigner shape [35]. Each of them is convolved with a resolution function obtained from simulated $\Sigma_b^{(*)-}$ decays, and is parameterized as the sum of three Gaussian distributions with a common mean. The average resolution is 1.97 MeV/c^2 for Σ_b^- and 2.25 MeV/c^2 for Σ_b^{*-}. The $\Sigma^{(*)\pm}$ masses and natural widths are freely varied in the fit to data, but the Gaussian widths are fixed and include a scale factor of 1.10, as indicated previously. The masses and widths of the $\Sigma_b^{(*)\pm}$ resonances are being studied in a separate analysis.

The combinatorial background is described by the threshold function

$$f_{\rm back}(\delta m) \propto (\delta m)^A (1 - e^{-\delta m/C}), \tag{2}$$

where the parameters A and C are freely varied in the fit to data. One set of parameters is used for the low-S/B region, and a separate set for the high-S/B region. For each S/B region, the RS and WS spectra share a common set of parameters.

The resulting mass fits are shown in Fig. 2. The $\Sigma_b^\pm$ and $\Sigma_b^{*\pm}$ signals appear prominently, and are constrained by the data in the low-S/B spectra (top pair of plots). The data show an enhancement at the expected δm value for the $\Xi_b^- \to \Lambda_b^0 \pi^-$ decay in the RS high-S/B region, but no such excess is seen in the corresponding WS sample. The total fitted signal yields for the RS and WS samples are 103 ± 33 and -7 ± 28, respectively.

The relative efficiency between the normalization and signal modes can be expressed as

$$\epsilon_{\rm rel} \equiv \frac{\epsilon_{\Lambda_b^0}}{\epsilon_{\Xi_b^-}} = \frac{\epsilon_{\rm rel}^{\rm acc} \epsilon_{\rm rel}^{\rm rec} \epsilon_{\rm rel}^{\rm BDT1,2}}{\epsilon_{\Xi_b^-\text{-only}}}, \tag{3}$$

where $\epsilon_{\rm rel}^{\rm acc} = 1.03 \pm 0.01$ is the relative efficiency for all of the stable daughter particles to be within the LHCb acceptance, $\epsilon_{\rm rel}^{\rm rec} = 1.38 \pm 0.02$ is the relative efficiency for reconstruction and selection, including the $p_T > 100$ MeV/c requirement on the π^- meson, $\epsilon_{\rm rel}^{\rm BDT1,2} = 1.00 \pm 0.01$ is the relative efficiency of the BDT1 and BDT2 selections, and $\epsilon_{\Xi_b^-\text{-only}} = 0.95 \pm 0.01$ includes the BDT3 requirement and the PID selection criteria on the π^- candidate. The relative efficiencies are obtained from simulated $\Xi_b^- \to \Lambda_b^0 \pi^-$ events and inclusively produced

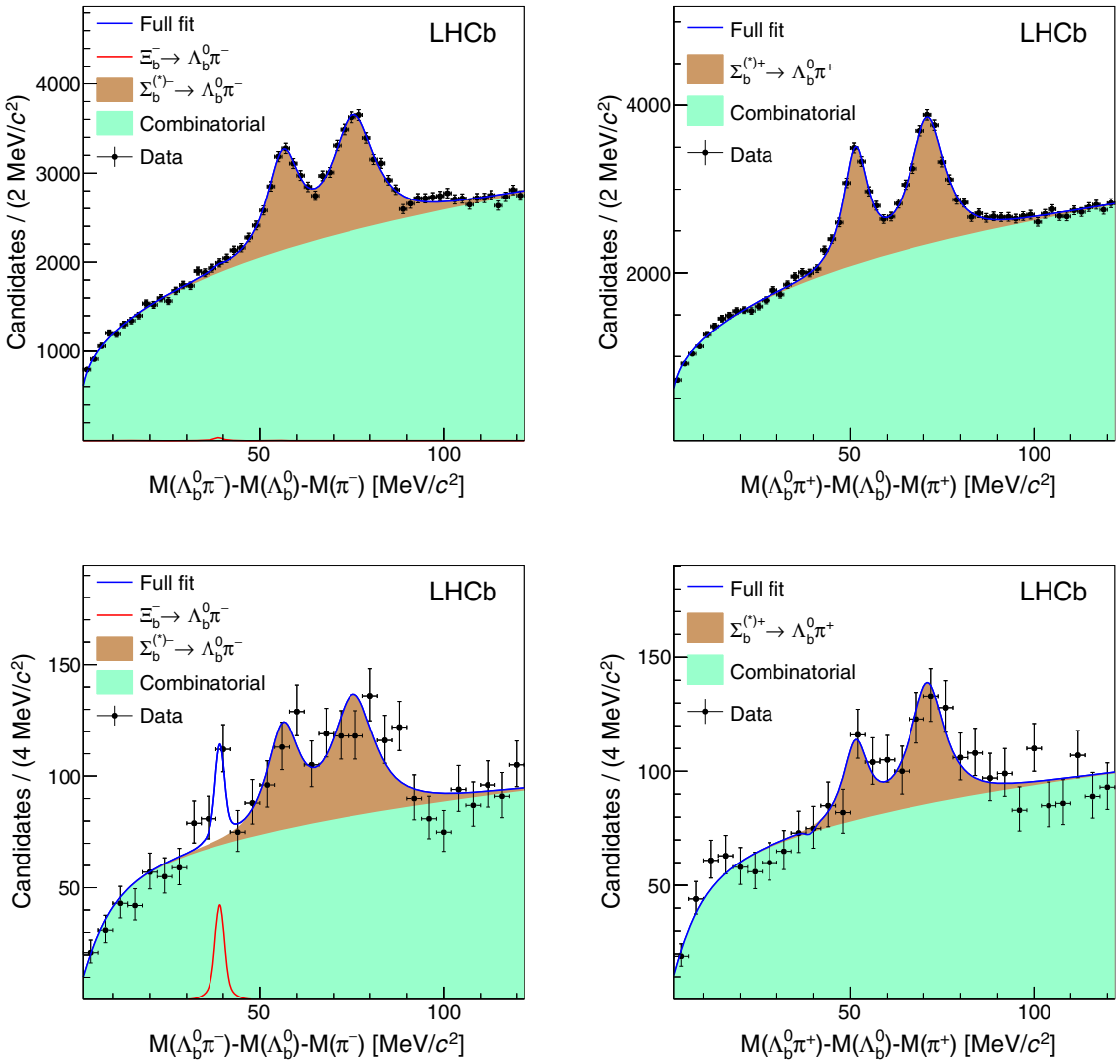

FIG. 2 (color online). Fit to the δm spectra in data: (top left) RS low S/B, (top right) WS low S/B, (bottom left) RS high S/B, and (bottom right) WS high S/B.

$\Lambda_b^0 \to \Lambda_c^+\pi^-$ decays, except for the PID requirements, which are taken from $D^{*+} \to D^0\pi^+$ calibration data. The relative efficiency is, therefore, 1.47 ± 0.03.

Several sources of systematic uncertainty affect the signal yield determination and thus the signal significance. Additional sources of systematic uncertainty contribute to the determination of r_s. The uncertainties are summarized in Table I. In the default fit, the Ξ_b^- signal peak position is fixed to the nominal value of $\delta m = 38.8$ MeV$/c^2$, which has an uncertainty of 0.5 MeV$/c^2$. We therefore refit the data with the peak position shifted by ± 0.5 MeV$/c^2$, obtaining changes of -6.4% and $+4.9\%$ in the yield. These values are assigned as a systematic error. Uncertainty in the signal yield due to the fixed mass resolution scale factor of 1.10 is investigated by varying it by ± 0.05, and we assign the average change in yield of 3.0% as a systematic error. Variations in the corresponding scale factor for the $\Sigma_b^{(*)-}$ resonances were investigated, and were found to have negligible impact on the $\Xi_b^- \to \Lambda_b^0\pi^-$ signal yield. Different choices for the fit range and the combinatorial background function were investigated; among these fit variations, a maximum shift in the signal yield of 12.6% was found. The full difference is assigned as a systematic uncertainty.

Additional systematic uncertainties that affect r_s include the relative efficiency between the low- and high-S/B regions, the slow π^- detection efficiency, and the yield of Λ_b^0 decays. In comparing the BDT1 distributions for $\Lambda_b^0 \to \Lambda_c^+\pi^-$ signal in data and simulation, as well as the background distributions for BDT3 in data and simulation, the relative efficiencies do not vary by more than 2% for any BDT selection. We therefore assign 2% as a systematic uncertainty. The π^- meson from the Ξ_b^- decay must be reconstructed and must have $p_T > 100$ MeV$/c$. The tracking efficiency uncertainty is assessed using data-driven techniques [36], and is less than 1.6%. The uncertainty due to the p_T requirement is estimated by

TABLE I. Relative systematic uncertainties (in percent) on the signal yield determination and on the quantity $(f_{\Xi_b^-}/f_{\Lambda_b^0})\mathcal{B}\times(\Xi_b^- \to \Lambda_b^0\pi^-)$, as described in the text.

Source	Value (%)
Mean δm	$^{+4.9}_{-6.4}$
Signal resolution	3.0
Combinatorial background shape	12.6
$\epsilon(\text{high}S/B)/\epsilon(\text{low}S/B)$	2.0
Slow π^- efficiency	2.3
Λ_b^0 normalization mode yield	1.0
Simulated sample size	2.1
Total for signal significance	$^{+13.9}_{-14.5}$
Total for r_s	$^{+14.4}_{-15.0}$

interpolating the p_T spectrum from 100 MeV/c to zero in simulated decays, and assuming that the fraction of signal events in this p_T region in data could differ from the simulated fraction by as much as 25%. This leads to a model uncertainty of 1.7%. Thus, an uncertainty of 2.3% is assigned to the detection of the π^- from the Ξ_b^- decay.

For the number of Λ_b^0 signal events, we assign a 1.0% uncertainty, which includes both the statistical component and a systematic uncertainty due to the signal and background shapes used to fit the $\Lambda_c^+\pi^-$ mass spectrum.

To check the robustness of the signal, the data were partitioned into different subsamples and the fitted yields in each were determined independently. The subsamples consisted of only 2012 data ($\sim 2/3$ of the data set), only negative magnet polarity data ($\sim$50% of the data sample), and only $\Lambda_b^0\pi^-$ data, not $\bar{\Lambda}\,{}_b^0\pi^+$ (expected to be $\sim$50%). In all three cases, the signal yields are compatible with expectations. Other robustness checks were also performed, such as placing a stringent PID requirement on the π^-, fitting only the RS data, and using only raw invariant masses (without the full kinematic fit). Upward and downward variations are observed, but in all cases, the fitted yields are consistent with expectations.

The significance of the signal is computed with Wilks's theorem [37]. The systematic uncertainty is included by convolving the likelihood function with a bifurcated Gaussian distribution whose widths are given by the asymmetric uncertainties in Table I, which leads to a significance of 3.2σ. We thus have evidence for the $\Xi_b^- \to \Lambda_b^0\pi^-$ decay.

With the yields and relative efficiencies presented previously, we find

$$\frac{f_{\Xi_b^-}}{f_{\Lambda_b^0}}\mathcal{B}(\Xi_b^- \to \Lambda_b^0\pi^-) = (5.7 \pm 1.8^{+0.8}_{-0.9}) \times 10^{-4},$$

where the uncertainties are statistical and systematic, respectively. To assess what this value implies in terms of $\mathcal{B}(\Xi_b^- \to \Lambda_b^0\pi^-)$, we consider a plausible range for $f_{\Xi_b^-}/f_{\Lambda_b^0}$ from 0.1–0.3, based on measured production rates of other strange particles relative to their nonstrange counterparts [19,38–41]. Assuming $f_{\Xi_b^-}/f_{\Lambda_b^0}$ is bounded between 0.1 and 0.3, the branching fraction $\mathcal{B}(\Xi_b^- \to \Lambda_b^0\pi^-)$ would be in the range from $(0.57 \pm 0.21)\%$ to $(0.19 \pm 0.07)\%$.

In summary, we present the first evidence for the $\Xi_b^- \to \Lambda_b^0\pi^-$ decay, which is mediated by the weak transition of the s quark. With the above assumptions for $f_{\Xi_b^-}/f_{\Lambda_b^0}$, the measured value for $\mathcal{B}(\Xi_b^- \to \Lambda_b^0\pi^-)$ is consistent with the range of 0.19%–0.76%, predicted in Ref. [14] assuming the diquark transitions have roughly the same weak amplitude as in B, D, and K meson decays. The results are also consistent with the value of 0.57%–0.62%, obtained using either a current algebra or pole-model approach, but are inconsistent with the values of 0.01% and 0.012% using the factorization approximation or the quark line approach [16]. The measured value of $\mathcal{B}(\Xi_b^- \to \Lambda_b^0\pi^-)$ disfavors a large enhancement to the decay rate of Ξ_b^- baryons from the $s \to u\bar{u}d$ transition, which could occur if the short-distance correlations within the $J^P = 0^+$ diquark system are enhanced, as suggested in Refs. [13,17,18].

We express our gratitude to our colleagues in the CERN accelerator departments for the excellent performance of the LHC. We thank the technical and administrative staff at the LHCb institutes. We acknowledge support from CERN and from the national agencies: CAPES, CNPq, FAPERJ, and FINEP (Brazil), NSFC (China), CNRS/IN2P3 (France), BMBF, DFG, and MPG (Germany), INFN (Italy), FOM and NWO (Netherlands), MNiSW and NCN (Poland), MEN/IFA (Romania), MinES and FANO (Russia), MinECo (Spain), SNSF and SER (Switzerland), NASU (Ukraine), STFC (United Kingdom), and NSF (USA). We acknowledge the computing resources that are provided by CERN, IN2P3 (France), KIT and DESY (Germany), INFN (Italy), SURF (Netherlands), PIC (Spain), GridPP (United Kingdom), RRCKI (Russia), CSCS (Switzerland), IFIN-HH (Romania), CBPF (Brazil), PL-GRID (Poland), and OSC (USA). We are indebted to the communities behind the multiple open-source software packages on which we depend. We are also thankful for the computing resources and the access to software R&D tools provided by Yandex LLC (Russia). Individual groups or members have received support from AvH Foundation (Germany), EPLANET, Marie Skłodowska-Curie Actions, and ERC (European Union), Conseil Général de Haute-Savoie, Labex ENIGMASS, and OCEVU, Région Auvergne (France), RFBR (Russia), GVA, XuntaGal, and GENCAT (Spain), and the Royal Society and Royal Commission for the Exhibition of 1851 (United Kingdom).

[1] V. A. Khoze and M. A. Shifman, Heavy quarks, Sov. Phys. Usp. **26**, 387 (1983).

[2] I. I. Bigi and N. G. Uraltsev, Gluonic enhancements in nonspectator beauty decays—An inclusive mirage though an exclusive possibility, Phys. Lett. B **280**, 271 (1992).

[3] I. I. Bigi, N. G. Uraltsev, and A. I. Vainshtein, Nonperturbative corrections to inclusive beauty and charm decays: QCD versus phenomenological models, Phys. Lett. B **293**, 430 (1992); **297**, 477(E) (1992).

[4] B. Blok and M. Shifman, The rule of discarding $1/N_c$ in inclusive weak decays (I), Nucl. Phys. **B399**, 441 (1993).

[5] B. Blok and M. Shifman, The rule of discarding $1/N_c$ in inclusive weak decays (II), Nucl. Phys. **B399**, 459 (1993).

[6] M. Neubert, B decays and the heavy-quark expansion, Adv. Ser. Dir. High Energy Phys. **15**, 239 (1998).

[7] N. Uraltsev, Heavy quark expansion in beauty and its decays, in Heavy Flavour Physics: A Probe of Nature's Grand Design, *Proceedings of the International School of Physics "Enrico Fermi," Course CXXXVII* (IOS Press, Amsterdam, 1998).

[8] G. Bellini, I. I. Y. Bigi, and P. J. Dornan, Lifetimes of charm and beauty hadrons, Phys. Rep. **289**, 1 (1997).

[9] R. Aaij *et al.* (LHCb Collaboration), Precision measurement of the ratio of the Λ_b^0 to $\bar{B}^0$ lifetimes, Phys. Lett. B **734**, 122 (2014).

[10] R. Aaij *et al.* (LHCb Collaboration), Measurement of the Ξ_b^- and Ω_b^- baryon lifetimes, Phys. Lett. B **736**, 154 (2014).

[11] R. Aaij *et al.* (LHCb Collaboration), Precision Measurement of the Mass and Lifetime of the Ξ_b^0 Baryon, Phys. Rev. Lett. **113**, 032001 (2014).

[12] R. Aaij *et al.* (LHCb Collaboration), Precision Measurement of the Mass and Lifetime of the Ξ_b^- Baryon, Phys. Rev. Lett. **113**, 242002 (2014).

[13] X. Li and M. B. Voloshin, Decays $\Xi_b \to \Lambda_b \pi$ and diquark correlations in hyperons, Phys. Rev. D **90**, 033016 (2014).

[14] S. Faller and T. Mannel, Light quark decays in heavy hadrons, Phys. Lett. B **750**, 653 (2015).

[15] M. B. Voloshin, Weak decays $\Xi_Q \to \Lambda_Q \pi$, Phys. Lett. B **476**, 297 (2000).

[16] S. Sinha and M. P. Khanna, Beauty-conserving strangeness-changing two-body hadronic decays of beauty baryons, Mod. Phys. Lett. A **14**, 651 (1999).

[17] M. Shifman and A. Vainshtein, Remarks on diquarks, strong binding and a large hidden QCD scale, Phys. Rev. D **71**, 074010 (2005).

[18] H. G. Dosch, M. Jamin, and B. Stech, Diquarks, QCD sum rules and weak decays, Z. Phys. C **42**, 167 (1989).

[19] K. A. Olive *et al.* (Particle Data Group), Review of particle physics, Chin. Phys. C **38**, 090001 (2014).

[20] A. A. Alves, Jr. *et al.* (LHCb Collaboration), The LHCb detector at the LHC, J. Instrum. **3**, S08005 (2008).

[21] M. Adinolfi *et al.*, Performance of the LHCb RICH detector at the LHC, Eur. Phys. J. C **73**, 2431 (2013).

[22] A. A. Alves, Jr. *et al.*, Performance of the LHCb muon system, J. Instrum. **8**, P02022 (2013).

[23] R. Aaij *et al.*, The LHCb trigger and its performance in 2011, J. Instrum. **8**, P04022 (2013).

[24] V. V. Gligorov and M. Williams, Efficient, reliable and fast high-level triggering using a bonsai boosted decision tree, J. Instrum. **8**, P02013 (2013).

[25] T. Sjöstrand, S. Mrenna, and P. Skands, A brief introduction to PYTHIA 8.1, Comput. Phys. Commun. **178**, 852 (2008).

[26] I. Belyaev *et al.*, Handling of the generation of primary events in Gauss, the LHCb simulation framework, J. Phys. Conf. Ser. **331**, 032047 (2011).

[27] D. J. Lange, The EvtGen particle decay simulation package, Nucl. Instrum. Methods Phys. Res., Sect. A **462**, 152 (2001).

[28] P. Golonka and Z. Was, PHOTOS Monte Carlo: A precision tool for QED corrections in Z and W decays, Eur. Phys. J. C **45**, 97 (2006).

[29] J. Allison *et al.* (Geant4 Collaboration), Geant4 developments and applications, IEEE Trans. Nucl. Sci. **53**, 270 (2006); S. Agostinelli *et al.* (Geant4 Collaboration), Geant4: A simulation toolkit, Nucl. Instrum. Methods Phys. Res., Sect. A **506**, 250 (2003).

[30] M. Clemencic, G. Corti, S. Easo, C. R. Jones, S. Miglioranzi, M. Pappagallo, and P. Robbe, The LHCb simulation application, Gauss: Design, evolution and experience, J. Phys. Conf. Ser. **331**, 032023 (2011).

[31] W. D. Hulsbergen, Decay chain fitting with a Kalman filter, Nucl. Instrum. Methods Phys. Res., Sect. A **552**, 566 (2005).

[32] L. Breiman, J. H. Friedman, R. A. Olshen, and C. J. Stone, *Classification and Regression Trees* (Wadsworth International Group, Belmont, CA, 1984).

[33] R. E. Schapire and Y. Freund, A decision-theoretic generalization of on-line learning and an application to boosting, J. Comput. Syst. Sci. **55**, 119 (1997).

[34] LHCb Collaboration, A search for time-integrated CP violation in $D^0 \to K^-K^+$ and $D^0 \to \pi^-\pi^+$ decays, CERN Report No. LHCb-CONF-2013-003.

[35] J. D. Jackson, Remarks on the phenomenological analysis of resonances, Nuovo Cimento **34**, 1644 (1964).

[36] R. Aaij *et al.* (LHCb Collaboration), Measurement of the track reconstruction efficiency at LHCb, J. Instrum. **10**, P02007 (2015).

[37] S. S. Wilks, The large-sample distribution of the likelihood ratio for testing composite hypotheses, Ann. Math. Stat. **9**, 60 (1938).

[38] R. Aaij *et al.* (LHCb Collaboration), Measurement of prompt hadron production ratios in pp collisions at $\sqrt{s} =$ 0.9 and 7 TeV, Eur. Phys. J. C **72**, 2168 (2012).

[39] R. Aaij *et al.* (LHCb Collaboration), Prompt charm production in pp collisions at $\sqrt{s} = 7$ TeV, Nucl. Phys. **B871**, 1 (2013).

[40] R. Aaij *et al.* (LHCb Collaboration), Measurement of the fragmentation fraction ratio f_s/f_d and its dependence on B meson kinematics, J. High Energy Phys. 04 (2013) 001.

[41] R. Aaij *et al.* (LHCb Collaboration), Measurements of prompt charm production cross-sections in pp collisions at $\sqrt{s} = 13$ TeV, CERN Report No. LHCb-PAPER-2015-041 (to be published).

R. Aaij,[38] C. Abellán Beteta,[40] B. Adeva,[37] M. Adinolfi,[46] A. Affolder,[52] Z. Ajaltouni,[5] S. Akar,[6] J. Albrecht,[9] F. Alessio,[38] M. Alexander,[51] S. Ali,[41] G. Alkhazov,[30] P. Alvarez Cartelle,[53] A. A. Alves Jr.,[57] S. Amato,[2] S. Amerio,[22] Y. Amhis,[7] L. An,[3] L. Anderlini,[17] J. Anderson,[40] G. Andreassi,[39] M. Andreotti,[16,a] J. E. Andrews,[58] R. B. Appleby,[54] O. Aquines Gutierrez,[10] F. Archilli,[38] P. d'Argent,[11] A. Artamonov,[35] M. Artuso,[59] E. Aslanides,[6] G. Auriemma,[25,b] M. Baalouch,[5] S. Bachmann,[11] J. J. Back,[48] A. Badalov,[36] C. Baesso,[60] W. Baldini,[16,38] R. J. Barlow,[54] C. Barschel,[38] S. Barsuk,[7] W. Barter,[38] V. Batozskaya,[28] V. Battista,[39] A. Bay,[39] L. Beaucourt,[4] J. Beddow,[51] F. Bedeschi,[23] I. Bediaga,[1] L. J. Bel,[41] V. Bellee,[39] N. Belloli,[20,c] I. Belyaev,[31] E. Ben-Haim,[8] G. Bencivenni,[18] S. Benson,[38] J. Benton,[46] A. Berezhnoy,[32] R. Bernet,[40] A. Bertolin,[22] M.-O. Bettler,[38] M. van Beuzekom,[41] A. Bien,[11] S. Bifani,[45] P. Billoir,[8] T. Bird,[54] A. Birnkraut,[9] A. Bizzeti,[17,d] T. Blake,[48] F. Blanc,[39] J. Blouw,[10] S. Blusk,[59] V. Bocci,[25] A. Bondar,[34] N. Bondar,[30,38] W. Bonivento,[15] S. Borghi,[54] M. Borisyak,[65] M. Borsato,[7] T. J. V. Bowcock,[52] E. Bowen,[40] C. Bozzi,[16,38] S. Braun,[11] M. Britsch,[11] T. Britton,[59] J. Brodzicka,[54] N. H. Brook,[46] E. Buchanan,[46] C. Burr,[54] A. Bursche,[40] J. Buytaert,[38] S. Cadeddu,[15] R. Calabrese,[16,a] M. Calvi,[20,c] M. Calvo Gomez,[36,e] P. Campana,[18] D. Campora Perez,[38] L. Capriotti,[54] A. Carbone,[14,f] G. Carboni,[24,g] R. Cardinale,[19,h] A. Cardini,[15] P. Carniti,[20,c] L. Carson,[50] K. Carvalho Akiba,[2,38] G. Casse,[52] L. Cassina,[20,c] L. Castillo Garcia,[38] M. Cattaneo,[38] Ch. Cauet,[9] G. Cavallero,[19] R. Cenci,[23,i] M. Charles,[8] Ph. Charpentier,[38] M. Chefdeville,[4] S. Chen,[54] S.-F. Cheung,[55] N. Chiapolini,[40] M. Chrzaszcz,[40] X. Cid Vidal,[38] G. Ciezarek,[41] P. E. L. Clarke,[50] M. Clemencic,[38] H. V. Cliff,[47] J. Closier,[38] V. Coco,[38] J. Cogan,[6] E. Cogneras,[5] V. Cogoni,[15,j] L. Cojocariu,[29] G. Collazuol,[22] P. Collins,[38] A. Comerma-Montells,[11] A. Contu,[15] A. Cook,[46] M. Coombes,[46] S. Coquereau,[8] G. Corti,[38] M. Corvo,[16,a] B. Couturier,[38] G. A. Cowan,[50] D. C. Craik,[48] A. Crocombe,[48] M. Cruz Torres,[60] S. Cunliffe,[53] R. Currie,[53] C. D'Ambrosio,[38] E. Dall'Occo,[41] J. Dalseno,[46] P. N. Y. David,[41] A. Davis,[57] O. De Aguiar Francisco,[2] K. De Bruyn,[6] S. De Capua,[54] M. De Cian,[11] J. M. De Miranda,[1] L. De Paula,[2] P. De Simone,[18] C.-T. Dean,[51] D. Decamp,[4] M. Deckenhoff,[9] L. Del Buono,[8] N. Déléage,[4] M. Demmer,[9] D. Derkach,[65] O. Deschamps,[5] F. Dettori,[38] B. Dey,[21] A. Di Canto,[38] F. Di Ruscio,[24] H. Dijkstra,[38] S. Donleavy,[52] F. Dordei,[11] M. Dorigo,[39] A. Dosil Suárez,[37] D. Dossett,[48] A. Dovbnya,[43] K. Dreimanis,[52] L. Dufour,[41] G. Dujany,[54] P. Durante,[38] R. Dzhelyadin,[35] A. Dziurda,[26] A. Dzyuba,[30] S. Easo,[49,38] U. Egede,[53] V. Egorychev,[31] S. Eidelman,[34] S. Eisenhardt,[50] U. Eitschberger,[9] R. Ekelhof,[9] L. Eklund,[51] I. El Rifai,[5] Ch. Elsasser,[40] S. Ely,[59] S. Esen,[11] H. M. Evans,[47] T. Evans,[55] A. Falabella,[14] C. Färber,[38] N. Farley,[45] S. Farry,[52] R. Fay,[52] D. Ferguson,[50] V. Fernandez Albor,[37] F. Ferrari,[14] F. Ferreira Rodrigues,[1] M. Ferro-Luzzi,[38] S. Filippov,[33] M. Fiore,[16,38,a] M. Fiorini,[16,a] M. Firlej,[27] C. Fitzpatrick,[39] T. Fiutowski,[27] K. Fohl,[38] P. Fol,[53] M. Fontana,[15] F. Fontanelli,[19,h] D. C. Forshaw,[59] R. Forty,[38] M. Frank,[38] C. Frei,[38] M. Frosini,[17] J. Fu,[21] E. Furfaro,[24,g] A. Gallas Torreira,[37] D. Galli,[14,f] S. Gallorini,[22] S. Gambetta,[50] M. Gandelman,[2] P. Gandini,[55] Y. Gao,[3] J. García Pardiñas,[37] J. Garra Tico,[47] L. Garrido,[36] D. Gascon,[36] C. Gaspar,[38] R. Gauld,[55] L. Gavardi,[9] G. Gazzoni,[5] D. Gerick,[11] E. Gersabeck,[11] M. Gersabeck,[54] T. Gershon,[48] Ph. Ghez,[4] S. Gianì,[39] V. Gibson,[47] O. G. Girard,[39] L. Giubega,[29] V. V. Gligorov,[38] C. Göbel,[60] D. Golubkov,[31] A. Golutvin,[53,38] A. Gomes,[1,k] C. Gotti,[20,c] M. Grabalosa Gándara,[5] R. Graciani Diaz,[36] L. A. Granado Cardoso,[38] E. Graugés,[36] E. Graverini,[40] G. Graziani,[17] A. Grecu,[29] E. Greening,[55] S. Gregson,[47] P. Griffith,[45] L. Grillo,[11] O. Grünberg,[63] B. Gui,[59] E. Gushchin,[33] Yu. Guz,[35,38] T. Gys,[38] T. Hadavizadeh,[55] C. Hadjivasiliou,[59] G. Haefeli,[39] C. Haen,[38] S. C. Haines,[47] S. Hall,[53] B. Hamilton,[58] X. Han,[11] S. Hansmann-Menzemer,[11] N. Harnew,[55] S. T. Harnew,[46] J. Harrison,[54] J. He,[38] T. Head,[39] V. Heijne,[41] K. Hennessy,[52] P. Henrard,[5] L. Henry,[8] E. van Herwijnen,[38] M. Heß,[63] A. Hicheur,[2] D. Hill,[55] M. Hoballah,[5] C. Hombach,[54] W. Hulsbergen,[41] T. Humair,[53] N. Hussain,[55] D. Hutchcroft,[52] D. Hynds,[51] M. Idzik,[27] P. Ilten,[56] R. Jacobsson,[38] A. Jaeger,[11] J. Jalocha,[55] E. Jans,[41] A. Jawahery,[58] M. John,[55] D. Johnson,[38] C. R. Jones,[47] C. Joram,[38] B. Jost,[38] N. Jurik,[59] S. Kandybei,[43] W. Kanso,[6] M. Karacson,[38] T. M. Karbach,[38,†] S. Karodia,[51] M. Kecke,[11] M. Kelsey,[59] I. R. Kenyon,[45] M. Kenzie,[38] T. Ketel,[42] E. Khairullin,[65] B. Khanji,[20,38,c] C. Khurewathanakul,[39] S. Klaver,[54] K. Klimaszewski,[28] O. Kochebina,[7] M. Kolpin,[11] I. Komarov,[39] R. F. Koopman,[42] P. Koppenburg,[41,38] M. Kozeiha,[5] L. Kravchuk,[33] K. Kreplin,[11] M. Kreps,[48] G. Krocker,[11] P. Krokovny,[34] F. Kruse,[9] W. Krzemien,[28] W. Kucewicz,[26,l] M. Kucharczyk,[26] V. Kudryavtsev,[34] A. K. Kuonen,[39] K. Kurek,[28] T. Kvaratskheliya,[31] D. Lacarrere,[38] G. Lafferty,[54,38] A. Lai,[15] D. Lambert,[50] G. Lanfranchi,[18] C. Langenbruch,[48] B. Langhans,[38] T. Latham,[48] C. Lazzeroni,[45] R. Le Gac,[6] J. van Leerdam,[41] J.-P. Lees,[4] R. Lefèvre,[5] A. Leflat,[32,38] J. Lefrançois,[7] E. Lemos Cid,[37] O. Leroy,[6] T. Lesiak,[26] B. Leverington,[11] Y. Li,[7] T. Likhomanenko,[65,64] M. Liles,[52] R. Lindner,[38] C. Linn,[38] F. Lionetto,[40] B. Liu,[15] X. Liu,[3] D. Loh,[48] I. Longstaff,[51] J. H. Lopes,[2] D. Lucchesi,[22,m] M. Lucio Martinez,[37] H. Luo,[50] A. Lupato,[22] E. Luppi,[16,a] O. Lupton,[55] A. Lusiani,[23] F. Machefert,[7] F. Maciuc,[29] O. Maev,[30] K. Maguire,[54] S. Malde,[55] A. Malinin,[64] G. Manca,[7] G. Mancinelli,[6] P. Manning,[59] A. Mapelli,[38] J. Maratas,[5]

J. F. Marchand,[4] U. Marconi,[14] C. Marin Benito,[36] P. Marino,[23,38,i] J. Marks,[11] G. Martellotti,[25] M. Martin,[6] M. Martinelli,[39] D. Martinez Santos,[37] F. Martinez Vidal,[66] D. Martins Tostes,[2] A. Massafferri,[1] R. Matev,[38] A. Mathad,[48] Z. Mathe,[38] C. Matteuzzi,[20] A. Mauri,[40] B. Maurin,[39] A. Mazurov,[45] M. McCann,[53] J. McCarthy,[45] A. McNab,[54] R. McNulty,[12] B. Meadows,[57] F. Meier,[9] M. Meissner,[11] D. Melnychuk,[28] M. Merk,[41] E Michielin,[22] D. A. Milanes,[62] M.-N. Minard,[4] D. S. Mitzel,[11] J. Molina Rodriguez,[60] I. A. Monroy,[62] S. Monteil,[5] M. Morandin,[22] P. Morawski,[27] A. Mordà,[6] M. J. Morello,[23,i] J. Moron,[27] A. B. Morris,[50] R. Mountain,[59] F. Muheim,[50] D. Müller,[54] J. Müller,[9] K. Müller,[40] V. Müller,[9] M. Mussini,[14] B. Muster,[39] P. Naik,[46] T. Nakada,[39] R. Nandakumar,[49] A. Nandi,[55] I. Nasteva,[2] M. Needham,[50] N. Neri,[21] S. Neubert,[11] N. Neufeld,[38] M. Neuner,[11] A. D. Nguyen,[39] T. D. Nguyen,[39] C. Nguyen-Mau,[39,n] V. Niess,[5] R. Niet,[9] N. Nikitin,[32] T. Nikodem,[11] A. Novoselov,[35] D. P. O'Hanlon,[48] A. Oblakowska-Mucha,[27] V. Obraztsov,[35] S. Ogilvy,[51] O. Okhrimenko,[44] R. Oldeman,[15,j] C. J. G. Onderwater,[67] B. Osorio Rodrigues,[1] J. M. Otalora Goicochea,[2] A. Otto,[38] P. Owen,[53] A. Oyanguren,[66] A. Palano,[13,o] F. Palombo,[21,p] M. Palutan,[18] J. Panman,[38] A. Papanestis,[49] M. Pappagallo,[51] L. L. Pappalardo,[16,a] C. Pappenheimer,[57] W. Parker,[58] C. Parkes,[54] G. Passaleva,[17] G. D. Patel,[52] M. Patel,[53] C. Patrignani,[19,h] A. Pearce,[54,49] A. Pellegrino,[41] G. Penso,[25,q] M. Pepe Altarelli,[38] S. Perazzini,[14,f] P. Perret,[5] L. Pescatore,[45] K. Petridis,[46] A. Petrolini,[19,h] M. Petruzzo,[21] E. Picatoste Olloqui,[36] B. Pietrzyk,[4] T. Pilař,[48] D. Pinci,[25] A. Pistone,[19] A. Piucci,[11] S. Playfer,[50] M. Plo Casasus,[37] T. Poikela,[38] F. Polci,[8] A. Poluektov,[48,34] I. Polyakov,[31] E. Polycarpo,[2] A. Popov,[35] D. Popov,[10,38] B. Popovici,[29] C. Potterat,[2] E. Price,[46] J. D. Price,[52] J. Prisciandaro,[37] A. Pritchard,[52] C. Prouve,[46] V. Pugatch,[44] A. Puig Navarro,[39] G. Punzi,[23,r] W. Qian,[4] R. Quagliani,[7,46] B. Rachwal,[26] J. H. Rademacker,[46] M. Rama,[23] M. Ramos Pernas,[37] M. S. Rangel,[2] I. Raniuk,[43] N. Rauschmayr,[38] G. Raven,[42] F. Redi,[53] S. Reichert,[54] M. M. Reid,[48] A. C. dos Reis,[1] S. Ricciardi,[49] S. Richards,[46] M. Rihl,[38] K. Rinnert,[52,38] V. Rives Molina,[36] P. Robbe,[7,38] A. B. Rodrigues,[1] E. Rodrigues,[54] J. A. Rodriguez Lopez,[62] P. Rodriguez Perez,[54] S. Roiser,[38] V. Romanovsky,[35] A. Romero Vidal,[37] J. W. Ronayne,[12] M. Rotondo,[22] T. Ruf,[38] P. Ruiz Valls,[66] J. J. Saborido Silva,[37] N. Sagidova,[30] P. Sail,[51] B. Saitta,[15,j] V. Salustino Guimaraes,[2] C. Sanchez Mayordomo,[66] B. Sanmartin Sedes,[37] R. Santacesaria,[25] C. Santamarina Rios,[37] M. Santimaria,[18] E. Santovetti,[24,g] A. Sarti,[18,q] C. Satriano,[25,b] A. Satta,[24] D. M. Saunders,[46] D. Savrina,[31,32] M. Schiller,[38] H. Schindler,[38] M. Schlupp,[9] M. Schmelling,[10] T. Schmelzer,[9] B. Schmidt,[38] O. Schneider,[39] A. Schopper,[38] M. Schubiger,[39] M.-H. Schune,[7] R. Schwemmer,[38] B. Sciascia,[18] A. Sciubba,[25,q] A. Semennikov,[31] N. Serra,[40] J. Serrano,[6] L. Sestini,[22] P. Seyfert,[20] M. Shapkin,[35] I. Shapoval,[16,43,a] Y. Shcheglov,[30] T. Shears,[52] L. Shekhtman,[34] V. Shevchenko,[64] A. Shires,[9] B. G. Siddi,[16] R. Silva Coutinho,[40] L. Silva de Oliveira,[2] G. Simi,[22] M. Sirendi,[47] N. Skidmore,[46] T. Skwarnicki,[59] E. Smith,[55,49] E. Smith,[53] I. T. Smith,[50] J. Smith,[47] M. Smith,[54] H. Snoek,[41] M. D. Sokoloff,[57,38] F. J. P. Soler,[51] F. Soomro,[39] D. Souza,[46] B. Souza De Paula,[2] B. Spaan,[9] P. Spradlin,[51] S. Sridharan,[38] F. Stagni,[38] M. Stahl,[11] S. Stahl,[38] S. Stefkova,[53] O. Steinkamp,[40] O. Stenyakin,[35] S. Stevenson,[55] S. Stoica,[29] S. Stone,[59] B. Storaci,[40] S. Stracka,[23,i] M. Straticiuc,[29] U. Straumann,[40] L. Sun,[57] W. Sutcliffe,[53] K. Swientek,[27] S. Swientek,[9] V. Syropoulos,[42] M. Szczekowski,[28] T. Szumlak,[27] S. T'Jampens,[4] A. Tayduganov,[6] T. Tekampe,[9] M. Teklishyn,[7] G. Tellarini,[16,a] F. Teubert,[38] C. Thomas,[55] E. Thomas,[38] J. van Tilburg,[41] V. Tisserand,[4] M. Tobin,[39] J. Todd,[57] S. Tolk,[42] L. Tomassetti,[16,a] D. Tonelli,[38] S. Topp-Joergensen,[55] N. Torr,[55] E. Tournefier,[4] S. Tourneur,[39] K. Trabelsi,[39] M. T. Tran,[39] M. Tresch,[40] A. Trisovic,[38] A. Tsaregorodtsev,[6] P. Tsopelas,[41] N. Tuning,[41,38] A. Ukleja,[28] A. Ustyuzhanin,[65,64] U. Uwer,[11] C. Vacca,[15,38,j] V. Vagnoni,[14] G. Valenti,[14] A. Vallier,[7] R. Vazquez Gomez,[18] P. Vazquez Regueiro,[37] C. Vázquez Sierra,[37] S. Vecchi,[16] J. J. Velthuis,[46] M. Veltri,[17,s] G. Veneziano,[39] M. Vesterinen,[11] B. Viaud,[7] D. Vieira,[2] M. Vieites Diaz,[37] X. Vilasis-Cardona,[36,e] V. Volkov,[32] A. Vollhardt,[40] D. Volyanskyy,[10] D. Voong,[46] A. Vorobyev,[30] V. Vorobyev,[34] C. Voß,[63] J. A. de Vries,[41] R. Waldi,[63] C. Wallace,[48] R. Wallace,[12] J. Walsh,[23] S. Wandernoth,[11] J. Wang,[59] D. R. Ward,[47] N. K. Watson,[45] D. Websdale,[53] A. Weiden,[40] M. Whitehead,[48] G. Wilkinson,[55,38] M. Wilkinson,[59] M. Williams,[38] M. P. Williams,[45] M. Williams,[56] T. Williams,[45] F. F. Wilson,[49] J. Wimberley,[58] J. Wishahi,[9] W. Wislicki,[28] M. Witek,[26] G. Wormser,[7] S. A. Wotton,[47] S. Wright,[47] K. Wyllie,[38] Y. Xie,[61] Z. Xu,[39] Z. Yang,[3] J. Yu,[61] X. Yuan,[34] O. Yushchenko,[35] M. Zangoli,[14] M. Zavertyaev,[10,t] L. Zhang,[3] Y. Zhang,[3] A. Zhelezov,[11] A. Zhokhov,[31] L. Zhong,[3] and S. Zucchelli[14]

(LHCb Collaboration)

[1]*Centro Brasileiro de Pesquisas Físicas (CBPF), Rio de Janeiro, Brazil*
[2]*Universidade Federal do Rio de Janeiro (UFRJ), Rio de Janeiro, Brazil*
[3]*Center for High Energy Physics, Tsinghua University, Beijing, China*
[4]*LAPP, Université Savoie Mont-Blanc, CNRS/IN2P3, Annecy-Le-Vieux, France*

[5]Clermont Université, Université Blaise Pascal, CNRS/IN2P3, LPC, Clermont-Ferrand, France
[6]CPPM, Aix-Marseille Université, CNRS/IN2P3, Marseille, France
[7]LAL, Université Paris-Sud, CNRS/IN2P3, Orsay, France
[8]LPNHE, Université Pierre et Marie Curie, Université Paris Diderot, CNRS/IN2P3, Paris, France
[9]Fakultät Physik, Technische Universität Dortmund, Dortmund, Germany
[10]Max-Planck-Institut für Kernphysik (MPIK), Heidelberg, Germany
[11]Physikalisches Institut, Ruprecht-Karls-Universität Heidelberg, Heidelberg, Germany
[12]School of Physics, University College Dublin, Dublin, Ireland
[13]Sezione INFN di Bari, Bari, Italy
[14]Sezione INFN di Bologna, Bologna, Italy
[15]Sezione INFN di Cagliari, Cagliari, Italy
[16]Sezione INFN di Ferrara, Ferrara, Italy
[17]Sezione INFN di Firenze, Firenze, Italy
[18]Laboratori Nazionali dell'INFN di Frascati, Frascati, Italy
[19]Sezione INFN di Genova, Genova, Italy
[20]Sezione INFN di Milano Bicocca, Milano, Italy
[21]Sezione INFN di Milano, Milano, Italy
[22]Sezione INFN di Padova, Padova, Italy
[23]Sezione INFN di Pisa, Pisa, Italy
[24]Sezione INFN di Roma Tor Vergata, Roma, Italy
[25]Sezione INFN di Roma La Sapienza, Roma, Italy
[26]Henryk Niewodniczanski Institute of Nuclear Physics Polish Academy of Sciences, Kraków, Poland
[27]AGH—University of Science and Technology, Faculty of Physics and Applied Computer Science, Kraków, Poland
[28]National Center for Nuclear Research (NCBJ), Warsaw, Poland
[29]Horia Hulubei National Institute of Physics and Nuclear Engineering, Bucharest-Magurele, Romania
[30]Petersburg Nuclear Physics Institute (PNPI), Gatchina, Russia
[31]Institute of Theoretical and Experimental Physics (ITEP), Moscow, Russia
[32]Institute of Nuclear Physics, Moscow State University (SINP MSU), Moscow, Russia
[33]Institute for Nuclear Research of the Russian Academy of Sciences (INR RAN), Moscow, Russia
[34]Budker Institute of Nuclear Physics (SB RAS) and Novosibirsk State University, Novosibirsk, Russia
[35]Institute for High Energy Physics (IHEP), Protvino, Russia
[36]Universitat de Barcelona, Barcelona, Spain
[37]Universidad de Santiago de Compostela, Santiago de Compostela, Spain
[38]European Organization for Nuclear Research (CERN), Geneva, Switzerland
[39]Ecole Polytechnique Fédérale de Lausanne (EPFL), Lausanne, Switzerland
[40]Physik-Institut, Universität Zürich, Zürich, Switzerland
[41]Nikhef National Institute for Subatomic Physics, Amsterdam, The Netherlands
[42]Nikhef National Institute for Subatomic Physics and VU University Amsterdam, Amsterdam, The Netherlands
[43]NSC Kharkiv Institute of Physics and Technology (NSC KIPT), Kharkiv, Ukraine
[44]Institute for Nuclear Research of the National Academy of Sciences (KINR), Kyiv, Ukraine
[45]University of Birmingham, Birmingham, United Kingdom
[46]H.H. Wills Physics Laboratory, University of Bristol, Bristol, United Kingdom
[47]Cavendish Laboratory, University of Cambridge, Cambridge, United Kingdom
[48]Department of Physics, University of Warwick, Coventry, United Kingdom
[49]STFC Rutherford Appleton Laboratory, Didcot, United Kingdom
[50]School of Physics and Astronomy, University of Edinburgh, Edinburgh, United Kingdom
[51]School of Physics and Astronomy, University of Glasgow, Glasgow, United Kingdom
[52]Oliver Lodge Laboratory, University of Liverpool, Liverpool, United Kingdom
[53]Imperial College London, London, United Kingdom
[54]School of Physics and Astronomy, University of Manchester, Manchester, United Kingdom
[55]Department of Physics, University of Oxford, Oxford, United Kingdom
[56]Massachusetts Institute of Technology, Cambridge, Massachusetts, USA
[57]University of Cincinnati, Cincinnati, Ohio, USA
[58]University of Maryland, College Park, Maryland, USA
[59]Syracuse University, Syracuse, New York, USA
[60]Pontifícia Universidade Católica do Rio de Janeiro (PUC-Rio), Rio de Janeiro, Brazil
(associated with Universidade Federal do Rio de Janeiro (UFRJ), Rio de Janeiro, Brazil)
[61]Institute of Particle Physics, Central China Normal University, Wuhan, Hubei, China
(associated with Center for High Energy Physics, Tsinghua University, Beijing, China)

[62]*Departamento de Fisica, Universidad Nacional de Colombia, Bogota, Colombia*
(associated with LPNHE, Université Pierre et Marie Curie, Université Paris Diderot, CNRS/IN2P3, Paris, France)
[63]*Institut für Physik, Universität Rostock, Rostock, Germany*
(associated with Physikalisches Institut, Ruprecht-Karls-Universität Heidelberg, Heidelberg, Germany)
[64]*National Research Centre Kurchatov Institute, Moscow, Russia*
(associated with Institute of Theoretical and Experimental Physics (ITEP), Moscow, Russia)
[65]*Yandex School of Data Analysis, Moscow, Russia*
(associated with Institute of Theoretical and Experimental Physics (ITEP), Moscow, Russia)
[66]*Instituto de Fisica Corpuscular (IFIC), Universitat de Valencia-CSIC, Valencia, Spain*
(associated with Universitat de Barcelona, Barcelona, Spain)
[67]*Van Swinderen Institute, University of Groningen, Groningen, The Netherlands*
(associated with Nikhef National Institute for Subatomic Physics, Amsterdam, Netherlands)

[†]Deceased.
[a]Also at Università di Ferrara, Ferrara, Italy.
[b]Also at Università della Basilicata, Potenza, Italy.
[c]Also at Università di Milano Bicocca, Milano, Italy.
[d]Also at Università di Modena e Reggio Emilia, Modena, Italy.
[e]Also at LIFAELS, La Salle, Universitat Ramon Llull, Barcelona, Spain.
[f]Also at Università di Bologna, Bologna, Italy.
[g]Also at Università di Roma Tor Vergata, Roma, Italy.
[h]Also at Università di Genova, Genova, Italy.
[i]Also at Scuola Normale Superiore, Pisa, Italy.
[j]Also at Università di Cagliari, Cagliari, Italy.
[k]Also at Universidade Federal do Triângulo Mineiro (UFTM), Uberaba-MG, Brazil.
[l]Also at AGH—University of Science and Technology, Faculty of Computer Science, Electronics and Telecommunications, Kraków, Poland.
[m]Also at Università di Padova, Padova, Italy.
[n]Also at Hanoi University of Science, Hanoi, Viet Nam.
[o]Also at Università di Bari, Bari, Italy.
[p]Also at Università degli Studi di Milano, Milano, Italy.
[q]Also at Università di Roma La Sapienza, Roma, Italy.
[r]Also at Università di Pisa, Pisa, Italy.
[s]Also at Università di Urbino, Urbino, Italy.
[t]Also at P.N. Lebedev Physical Institute, Russian Academy of Science (LPI RAS), Moscow, Russia.